# Comparison of Spectrally Narrow-Band Capture Versus Wide-Band with a Priori Sample Analysis for Spectral Reflectance Estimation

*Francisco H. Imai, Mitchell R. Rosen and Roy S. Berns*
*Munsell Color Science Laboratory, Rochester Institute of Technology*
*Rochester, New York*

## Abstract

Two alternative systems for spectral reconstruction of scene reflectances are compared. Both approaches utilize a CCD camera modulated by a set of filters after which a system model is applied to derive a pixel-by-pixel estimation of scene reflectance spectra. The qualitative difference between the filter sets for the pair of approaches warrants the current comparison. The first approach, described in terms of spectral band pass, uses a set of minimally redundant filters extreme in contrast which pass highly localized radiation. The second approach is based on a set of shaped non-selective filters. Theoretically, an ideal implementation of the first, narrow-band, approach should deliver accurate reflectance estimation for any scene object, independent of the characterization scheme used to build the system model. The second, wide-band, approach has theoretical dependence on the relationship between scene colorants and system model assumptions. When *a priori* knowledge of the expected colorant makeup of a scene is used to steer the choice of color samples from which the system model is derived, the expected robustness of the wide-band approach is theoretically improved. Results from implementations of the two approaches are contrasted and differences between theoretical expectations and those obtained are discussed.

## Introduction

It is widely known that conventional techniques of photography and scanning rely on metamerism. Although these techniques can produce pleasant reproductions, they are shown to exercise inadequate control over colorimetric error for certain quality critical applications, such as artwork reproduction.[1-4] Except for highly constrained examples, reconstructing spectra from such imaging systems is an arbitrary process with no expectation of accuracy. The number of digital archives for museum collections has increased exponentially in the past few years. Traditional trichromatic methods extensively used by these archives for capturing and storing images suffer from metameric limitations. This lack of fidelity is particularly noticeable when one makes a side by side comparison between an original object and its reproduction. The European museum community has invested considerable energy toward addressing the limitations of trichromatic-based image acquisition systems. A seven-channel digital camera has been developed and employed at such installations as The National Gallery (London, England) and the Uffizi Gallery (Florence, Italy). This benchmark program is called VASARI (Visual Arts System for Archiving and Retrieval of images).[5] From our viewpoint, a significant drawback is that the captured multi-spectral information is used only to create a direct mapping to a colorimetric three-dimensional space. Since spectral reconstruction is the only way to ensure a color match for all observers and across changes in illumination, it would be advantageous to build a system which maps to spectra rather than colorimetry.

The Munsell Color Science Laboratory has been developing implementations of end-to-end scene to hardcopy multi-spectral imaging systems.[6-10] Such a system would consist of an acquisition module,[9] an image processing module[8,10] and a spectral printing module.[8-12] At the previous Color Imaging Conference, we presented methods for wide-band multi-spectral imaging and spectral estimation which were based on the use of a typical trichromatic digital camera combined with either multiple scene illuminants or multiple camera filterings.[13,14] We also discussed implications of performing the spectral estimation in various color spaces, such as reflectance, Kubelka-Munk and new empirical spaces.[15] The presented methods produced reasonable results in terms of colorimetric and spectral accuracy giving a simple way to get spectral images without investing in much more than a common trichromatic system. In this paper, we are performing further analysis of wide-band approaches with comparison to narrow-band acquisition methods.

### Narrow-band Image Capture for Spectral Reflectance Estimation

The first and most direct method to capture spectral data is to increase the sampling increment above the traditional three channels using highly selective, spectrally

narrow filterings. In the limit, this would be equivalent to using a spectroradiometer to sample the visible spectrum at each pixel. With appropriate calibration, the system becomes a spatial spectrophotometer. In a similar vain, traditional trichromatic approaches can be seen as analogous to capturing a scene with a spatial densitometer or, at best, a spatial colorimeter. Various filtering technologies are available today which can produce spectrally narrow results. For these experiments a solid state liquid crystal tunable filter (LCTF)[8,16-18] was used. The LCTF has advantages of being solid-state and reliably repeatable, thus registration and calibration artifacts are not a concern between each filter setting. The LCTF is easily controllable from a computer making for an efficient, automated and relatively fast imaging environment. It has been accepted that the LCTF is free from spectral non-uniformities introduced from the angular sensitivities which are known to be associated with alternative technologies such as interference filters.[19]

Thirty-one LCTF filter settings were chosen for these experiments. Nominal center wavelengths ranged from 400nm to 700nm in increments of 10nm. Throughput and band pass width vary across the visible spectrum with efficiency being far lowest for the blue frequencies, peaking in the greens and decreasing somewhat for the reds. For building the system model, a five stage process is implemented. First, exposure metering is necessary to determine an integration time for each wavelength setting such that dynamic range is optimized but clipping is avoided. A second and third stage involve a white and dark calibration of the system for the chosen integration times. Success of the white calibration will be a major factor in determining the level of accuracy delivered for absolute scene reflectance reconstruction. For the fourth stage, an assortment of colors with known reflectances are placed in the scene and captured by the system. Finally the system model is built by determining the relationship between the white/dark corrected digital values for each filter setting and the sample reflectances associated with that filter setting. These stages are summarized in Figure 1. Because our 12-bit camera was operated only under conditions where it has a linear response, all system models were linear. Scene images captured under the same illumination conditions with the same filterings may be transformed to reflectance through use of the system model as illustrated in Figure 2.

One of the most important advantages to a narrow-band approach is its robustness to arbitrary spectral shapes. In the ideal implementation the spectral band pass of the filters is infinitesimally wide, and thus sampling theory would show that all features which are at least as wide as twice the sampling rate (2 x 10nm = 20nm, in this case) would be reconstructed perfectly. Of course, our own implementation is not ideal, as there is finite spectral width to our filters. But, to within approximations discussed later, our system does seek to approach such a sampling regime.
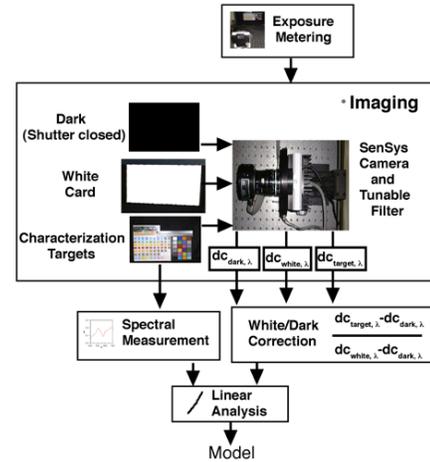


*Figure 1. Building System Model for Narrow-band spectral reflectance reconstruction.*

## Wide-band Image Capture for Spectral Reflectance Estimation

Because of the absorption characteristics of both man-made and natural colorants, it is unusual to encounter spectral features which are abrupt or very narrow. This is encouraging for wide-band approaches to reflectance reconstruction. Further, spectral analyses of colored stimuli using linear modeling techniques typically result in less than ten eigenvectors.[20-25] Five to eight basis vectors seem to be sufficient for an accurate spectral reconstruction of artwork. Thus one should be able to greatly reduce the number of necessary channels from the narrow-band 31 and still produce accurate spectra. A conventional trichromatic digital camera combined with a series of absorption filters can provide such a system.
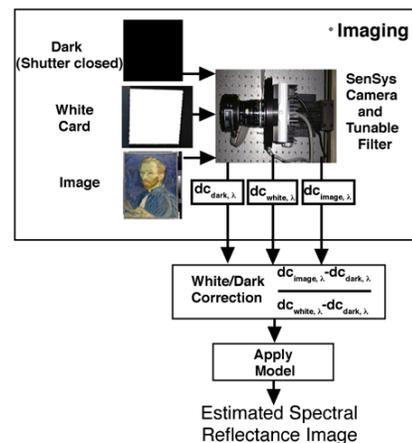


*Figure 2. Narrow-band spectral acquisition system*

Seven filter combinations were chosen for this approach. One was no filter at all placed in front of a three filter RGB color CCD camera and the other six combinations were a series of Wratten filters placed in front of the RGB camera. System modeling starts in similar fashion as the narrow-band approach. First light metering determines integration time. Second white calibration and third dark images are captured at each integration time. Again, for the fourth stage, an assortment of colors with known reflectances are placed in the scene and captured by the system. Here, theory says that color patches should consist of colorants which are similar to colorants which will comprise an eventual scene. White/dark corrected digital counts are compared to known reflectances and eigenvector analysis takes place resulting in the system model. These stages are summarized in Figure 3. Scene images captured under the same illumination conditions with the same filterings may be transformed to reflectance through use of the system model as illustrated in Figure 4.
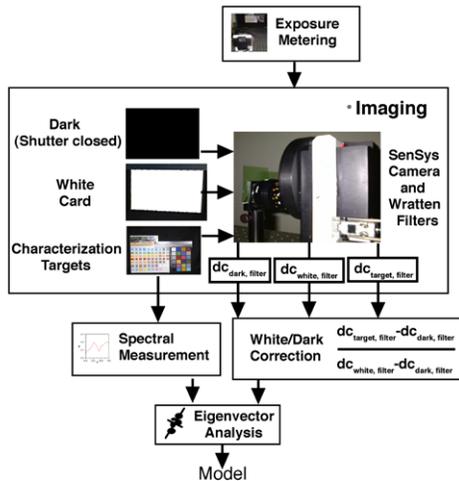


*Figure 3. Building System Model for Wide-band spectral reflectance reconstruction.*
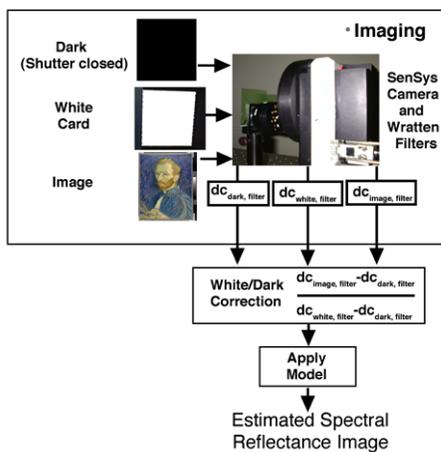


*Figure 4. Wide-band spectral acquisition with a priori analysis.*

## Experimental

We used a Photometrics SenSys monochrome CCD camera using a cooled grade 1 Kodak CCD type KAF1602E. The camera provides 1536 by 1024 resolution image, 12 bit linear data with linearity error of 0.07%. The camera has a filter wheel with R, G, B filters among other astronomical purpose filters such as IR and UV filters, in front of the CCD. Figure 5 shows the quantum efficiency of Sensys Camera.
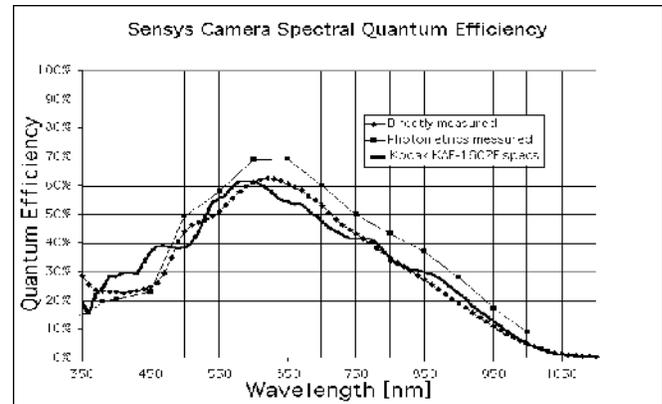


*Figure 5. Quantum Efficiency of Sensys Camera. Measurements made at the Munsell Lab are compared with Photometrics measurements provided with the camera as well as the Kodak specifications for the chip.*

Seven targets were selected to be imaged; the GretagMacbeth ColorChecker Rendition Chart, the large Kodak Q-14 Gray Scale (CAT 152 7662), a target made using 226 chips from the New Munsell Student Color Set[26] that we call Munsell Target, a poster-color painting of a flower arrangement and three painted patches set, one produced using poster-color paints (the same used for the flower arrangement painting) and two other produced using oil paints. The poster-color patches were painted using Cerulean Blue and Rose Violet manufactured by Sakura, Ultramarine, Permanent Yellow, Sap Green and Black manufactured by Pentel. The poster-color patches were coated with Krylon Kamar Varnish that is a non-yellowing protection. One of the oil painting targets, that we call Ross target (painted by Ross Merrill, a conservator working at the National Gallery of Art, Washington, D.C.) was created using 68 pigments representing blues, greens, yellows, reds, earth colors, browns and radiant colors that are among the most frequently used by artists. Another oil painting target, called van Gogh target, was created by Roy Berns comprising 106 patches created using 6 representative pigments of the colors present in one van Gogh self-portrait painted in 1889, part of the Whitney collection at the National Gallery of Art.[27]

The targets were imaged inside a Macbeth viewing booth Model PPM 01 that provides three different

illumination; daylight illuminant (two filtered Osram, FKT/EYH 250W, 120V G5.3 halogen lamps), A illuminant (four halogen lamps) and fluorescent illuminant (two ultramarine 3000 36T2 slimline lamps). The walls and the base of the viewing booth were covered with a black fabric to reduce flare. The targets were attached on the back wall of the viewing booth.

In the wide-band capture experiments, six different Kodak Wratten filters (light-blue filter 38, very light green filter 66, green color conversion filter cc50G, blue conversion filter 80B, yellow filter 06 and green filter 55) were used as external filters. Images were captured with each of the Wratten filters and one channel without any Wratten filter to generate seven triplets of R, G, B signals (obtained using the R, G, B filters present at the camera filter wheel). The seven R, G, B filtered triplets were captured for each of the three illuminants delivering a total of 63 different filter/illuminant combinations captured for each image. We believe that this collection of imaged conditions will provide a comprehensive database for analyzing multi-spectral imaging experiments in the future. In this article, we are going to focus on sets of six trichromatic signals using a combination of the R, G, B without external filter and with light-blue Wratten filter under the daylight illuminant. Principal component analyses were performed for the targets and a transformation was derived relating the digital counts to the eigenvalues of the eigenvectors.

In the case of the narrow-band capture, we used a C.R.I. Varispec solid state liquid crystal tunable filter (LCTF). This filter is manufactured by Cambridge Research and Instrumentation, Inc. (C.R.I). The filter has no moving parts. Selection of spectral band pass occurs through a change in electric field. Our filter was a high contrast model with a nominal band pass of 10nm. High contrast specifies average transmission of less than 0.1% of out of band wavelengths. Figure 6 shows measured transmittance of our filter. Multiple images were captured for settings of the tunable filter between 400nm and 720nm at every 5nm under both daylight and A illumination. For these discussions, only the images captured every 10nm under daylight are used, but the full set should be a valuable addition to the data base of wide-band images described above.

Colorimetric and spectral accuracy metrics such as $\Delta E^*_{94}$, spectral reflectance error rms factor and metamerism index have been commonly used to evaluate spectral estimation accuracy.[11,13-15] Color difference equations such as $\Delta E^*_{94}$ are defined for specific illuminant and observer and can produce misleading spectral accuracy metric between metameric matches. Spectral reflectance error rms factor we find to be inadequate at showing whether a reconstructed spectrum adheres to the original spectral curvature. The metamerism index is also limited in the sense that it is defined for particular color difference metrics, illuminants and observer. A metric we have chosen to use is the range of absolute reflectance error. Absolute error is computed as the difference between the

measured and the predicted spectral reflectance for each wavelength. The range is then defined as the difference between the maximum and minimum of the absolute spectral error. The smaller the range of absolute reflectance error, the more the reconstructed spectrum adheres to the curvature of the measured reflectance. We find it a desirable characteristic that this metric is highly sensitive to differences between measured and reconstructed spectral shape, but completely insensitive to lightness errors which are manafested as vertical spectral shifts. Alternative metrics can be utilized to recapture the lightness error, if desired. Different methods and filter combinations can be compared by calculating the number of patches of imaged targets that have error range smaller than a pre-determined range threshold. In this case we are going to use 10% as the absolute spectral error range threshold as our tolerance.
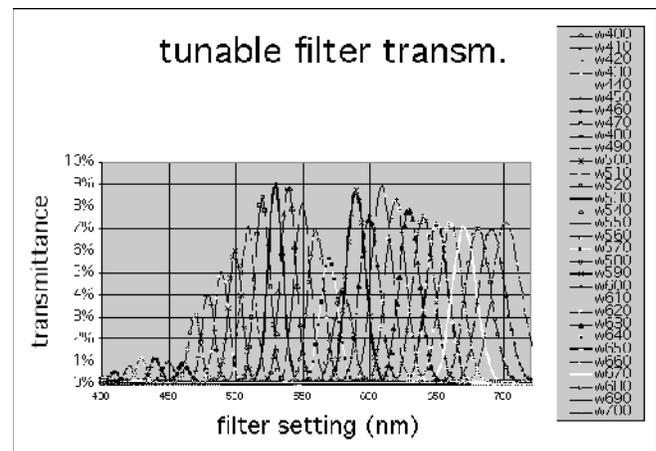


*Figure 6. Measured transmittances of the tunable filter at the 31 filter settings used for these experiments. Note that for wavelength settings less than 470nm, transmittances hover at and below 1%. Maximum transmittances are around 9%. Also note that band pass increases with increasing wavelength to a maximum FWHM of approximately 40nm.*

## Results and Discussion

Due to the non-uniformity of the illumination inside the viewing booth a white spatial correction was performed on a pixel-by-pixel basis. Figures 7 and 8 show images of white corrected targets with lines representing the distribution of digital signals within bands of values relative to the image of a white cardboard, respectively for wide-band imaging and narrow-band imaging under daylight illumination. We were surprised at the iso-signal signature which the narrow-band system delivered. The white correction stage of our imaging signal processing is designed to take into account and remove the effects of non-uniformities in illumination. Although the same step can also handle spatial non-uniformities in sensitivities and throughput of the camera system, when such corrections

become large, they increase quantization noise. Combining these findings with some of the subsequent reconstruction errors which appear to be spatially correlated, our suspicions were raised as to whether our tunable filter might not have spectral non-uniformities spatially as well.
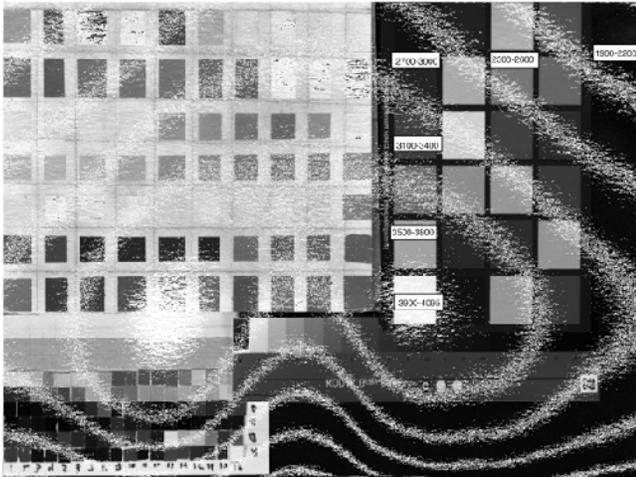


*Figure 7. Wide-band non-uniformity: lines indicate bands of iso-signal taken from the wide-band white image and superimposed on a target image. Note the two off-center "hot spots" of maximum signal. These hot spots are where maximum illumination is expected due to the set-up of the light booth.*



*Figure 8. Narrow-band non-uniformity: lines indicate bands of iso-signal taken from the narrow-band white image and superimposed on a target image. Note the single "hot spot" of maximum signal is now centered. Although these bands are slightly lobed, like those of the wide-band example, above, the tunable filter is heavily attenuating signal as objects move away from the center.*

For the wide-band acquisition approach, the Ross target was used as a training set to calculate 6 eigenvectors. The transformation from digital counts to reflectance obtained for the Ross Target was applied to the color checker used here as a verification target. The results in terms of ΔE*94 calculated for illuminant D50 and 2 degree observer as well as the percentage of patches whose estimated spectral was predicted within 10% of the absolute spectral error range are shown in Table I. The narrow-band approach theoretically could have used any combination of patches as long as the combined set had a wide range of reflectances across the wavelength range of interest. Since we were operating the CCD camera in its linear range, white and dark corrected patch digital values should have made straight lines in digit vs. measured reflectance. However some unexpected results were obtained for this narrow-band capture as shown in Figure 9.
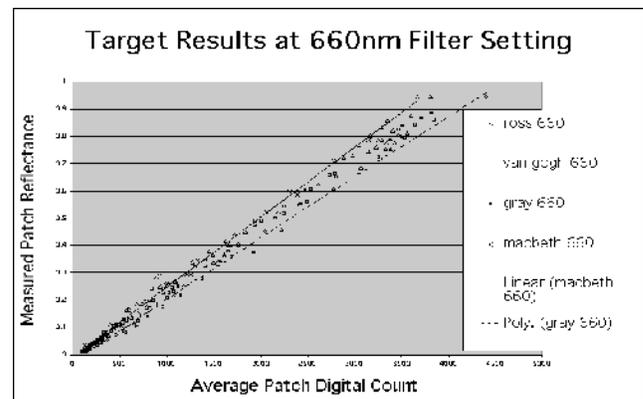


*Figure 9. Narrow-band unexpected results for example filter setting at 660nm. Ideal implementation would have resulted in a straight line relationship. Here, it shows that a range of reflectances are associated with the same white and dark corrected average patch digital counts.*

The most likely reason for these unexpected results is spatially related filter artifacts. Through analysis of our data, we found that when we limit ourselves to a spatial region which spans about 2/3 of image area, good results are obtained. See Figure 10. Good results are defined as those which produce a spectral error range of 10% or less.

Further, it was found that for the best average performance, the system model should be built using the 23 central patches outlined in Figure 11. The reasons for these spatially correlated performance issues is not fully understood yet. It is believed to be a combination of quantization noise introduced by the tunable filter which results from the radial falloff of transmittance and, secondly, a possible spectral leakage off center.
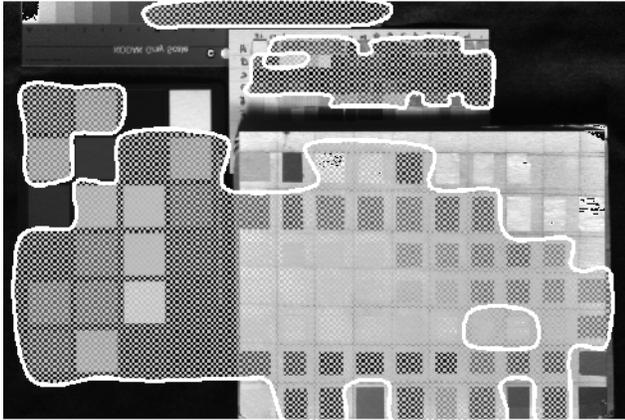
*Figure 10. Narrow-band region for relatively low spectral error ranges: shaded area.*
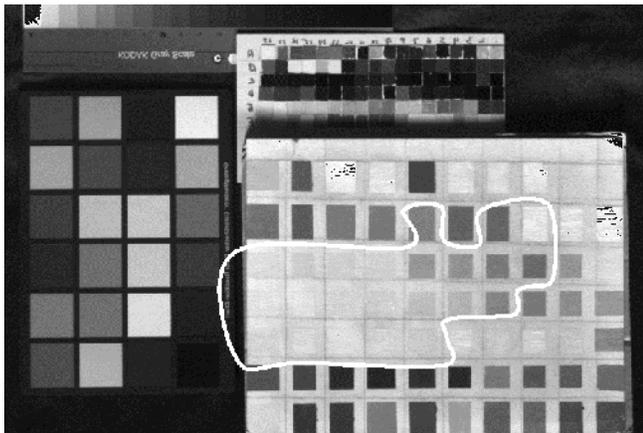


*Figure 11. Narrow-band patches used for creating system model with best average results. 23 circled patches comprise the set.*

**Table I. Wide-band results: Colorimetric and spectral differences between reconstructed and measured spectral reflectances**

| Results | Number of eigenvectors and Target used for eigenvector analysis | Mean $\Delta E^*_{94}$ (D50, 2°) | Max $\Delta E^*_{94}$ (D50, 2°) | Percentage of patches within 10% absolute spectral error range |
|---|---|---|---|---|
| Ross Target | 6 Ross | 1.9 | 5.2 | 79 |
| Color Checker | 6 Ross | 2.6 | 6.3 | 96 |

**Table II. Narrow-band results: Colorimetric and spectral differences between reconstructed and measured spectral reflectances**

| Results | Number of patches and Target used for building model | Mean $\Delta E^*_{94}$ (D50, 2°) | Max $\Delta E^*_{94}$ (D50, 2°) | Percentage of patches within 10% absolute spectral error range |
|---|---|---|---|---|
| Ross "Good Region" (see Fig. 10) | 23 Ross | 2.9 | 9.1 | 100 |
| Full Ross Target | 23 Ross | 3.4 | 9.1 | 78 |
| Color Checker | 23 Ross | 4.6 | 11.3 | 83 |
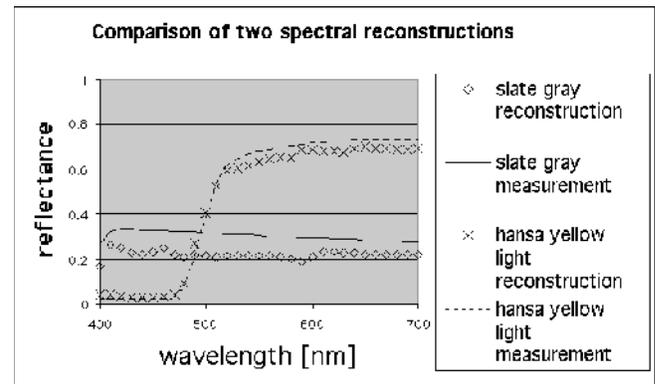


*Figure 12. Narrow-band spectral reconstruction results. Slate gray had high $\Delta E^*$, 9.1, but low spectral error range, 5.9%. Hansa yellow light had low $\Delta E^*$, 2.3, but high spectral error range, 10.6%.*

As mentioned earlier, low $\Delta E^*$ does not perfectly correlate with low spectral error range. In particular, if the $\Delta E^*$ is dominated by L* error, error range will be very low. For example, the reconstruction of the slate gray patch from the Ross target is illustrated in Figure 12. Here a relatively high $\Delta E^*$ of 9.1 is dominated by L* error. The spectral error range for this patch is 5.9%. The shape is well reconstructed, just at the wrong lightness. Hansa yellow light is another Ross patch with its reconstructions also illustrated in Figure 11. Here, although the $\Delta E^*$ is about one quarter of the slate gray patch at 2.3, its spectral error range is greater than 10%.

## Conclusion

Theoretically, a narrow-band approach for capturing and reconstructing spectral reflectances should be more robust than a wide band approach, especially when the constituent colorants for a scene are different than those in the sample set used to create the system model. For our examples here, we found that the opposite was actually true. The wide band approach had similar results in term of spectral error as the narrow band on the patch set for which the wide-band system model was tuned. But the wide-band results were superior to the narrow-band results for a second target for which the wide-band model was not designed.

We have theorized that a spatial anomaly in our narrow band filter has likely caused these unexpected results. We will further investigate this theory.

The database of images collected for this study should be useful for future spectral imaging investigations. The many combinations of illuminants and filters, both wide and narrow-band, will be very valuable for various studies and simulation projects.

## References

1. F. König and P. G. Herzog, On the Limitations of Metameric Imaging, in IS&Ts 1999 PICS Conference, IS&T, Springfield, VA, 1999, pp. 163-168.
2. F. Schmitt, H. Brettel, J. Y. Hardberg, Multispectral Imaging Development at ENST, in International Symposium on Multispectral Imaging and Color Reproduction for Digital Archives, Chiba, Japan, 1999, pp. 50-57.
3. B. Hill, Color capture, color management and the problem of metamerism: does multispectral imaging offer the solution? in Color Imaging: Device-Independent Color, Color Hardcopy, and Graphic Arts V, R. Eschbach, G. G. Marcu, Editors, Proc. of SPIE 3963 Bellingham, WA, 2000, pp.2-14.
4. R. S. Berns, Challenges for color science in multimedia imaging, in L. MacDonald and M. R. Luo, Eds., Colour Imaging: Vision and Technology, John Wiley & Sons, Chichester, 1998, pp. 99-127.
5. K. Martinze, J. Cupitt and D. Saunders, High resolution colorimetric imaging of paintings, in Cameras, Scanners, and Image Acquisition Systems, Proc. of SPIE 1901, Bellingham, WA, 1993, pp. 25-36.
6. R. S. Berns, F. H. Imai, P. D. Burns and Di-Y. Tzeng, Multi-spectral-based color reproduction research at the Munsell Color Science Laboratory, in Electronic Imaging: Processing, Printing, and Publishing in Color, Jan Bares, Editor, Proc. of SPIE 3409, Bellingham, WA, 1998, pp.14-25.
7. F. H. Imai and R. S. Berns, High-resolution Multi-Spectral Image Archives: A Hybrid Approach, in IS&T/SID Sixth Color Imaging Conference: Color Science, Systems, and Applications, IS&T, Springfield, VA, 1998, pp. 224-227.
8. M. Rosen, Lippmann2000: A spectral image database under construction, in International Symposium on Multispectral Imaging and Color Reproduction for Digital Archives, Chiba, Japan, 1999, pp. 117-122.
9. F. H. Imai, M. R. Rosen, R. S. Berns, and D. Tzeng, Spectral Reproduction from scene to Hardcopy I: Input and Output, submitted to Electronic Imaging, 2001.
10. M. R. Rosen, F. H. Imai X. Jiang and N. Ohta, Spectral Reproduction from scene to Hardcopy II: Image Processing, submitted to Electronic Imaging, 2001.
11. D. Tzeng, Spectral-Based Color Separation Algorithm Development for Multiple-Ink Color Reproduction, Ph.D. dissertation, R.I.T., Rochester, N.Y, 1999. Available at http://hering.cis.rit.edu/~dxt1649/thesis.pdf
12. D. Tzeng and R. S. Berns, Spectral-Based Six-Color Separation Minimizing Metamerism, in IS&T/SID Eighth Color Imaging Conference: Color Science, Systems, and Applications, IS&T, Springfield, VA, 2000.
13. F. H. Imai and R. S. Berns, A comparative analysis of spectral reflectance reconstruction in various spaces using a trichromatic camera system, in IS&T/SID Seventh Color Imaging Conference: Color Science, Systems, and Applications, IS&T, Springfield, VA, 1999, pp. 21-25.
14. F. H. Imai and R. S. Berns, Spectral Estimation Using Trichromatic Digital Cameras, in International Symposium on Multispectral Imaging and Color Reproduction for Digital Archives, Chiba, Japan, 1999, pp. 42-49.
15. F. H. Imai, R. S. Berns, and D. Tzeng, A Comparative Analysis of Spectral Reflectance Estimated in Various Spaces Using a Trichromatic Camera System. Journal of Imaging Science and Technology 44, 280-287 (2000).
16. S. Tominaga, Spectral Imaging by a Multi-Channel Camera, in IS&T/SPIE Conference on Color Imaging: Device-Independent Color, Color Hardcopy, and Graphic Arts IV, G. B. Beretta, and R. Eschbach, Editors, Proc. of SPIE 3648, Bellingham, WA, 1999, pp. 38-47.
17. J. Y. Hardeberg, F. J. Schmitt, H. Brettel, Multispectral image capture using a tunable filter, in Color Imaging: Device-Independent Color, Color Hardcopy, and Graphic Arts V, R. Eschbach, G. G. Marcu, Proc, of SPIE 3963 Bellingham, WA, 2000, pp.77-88.
18. R. W. Slawson, Z. Ninkov and E. P. Horch, Hyperspectral Imaging: Wide-area spectrophotometry using a liquid-crystal tunable filter, Publications of the Astronomical Society of the Pacific, 111, 621-626, (1999).
19. F. König and W. Præfke, The practice of multispectral image acquisition, in Electronic Imaging: Processing, Printing, and Publishing in Color, Jan Bares, Editor, Proceedings of SPIE 3409, Bellingham, WA, 1998, pp.34-41.
20. H. Haneishi, T. Hasegawa, N. Tsumura and Y. Miyake, Design of color filters for recording artworks, in IS&T's 50th Annual Conference, Springfield, VA, 1997, pp. 369-372.
21. Y. Miyake, Y. Yokoyama, N. Tsumura, H. Haneishi, K. Miyata and J. Hayashi, Development of multiband color imaging systems for recording of art paintings, in IS&T/SPIE Conference on Color Imaging: Device-Independent Color, Color Hardcopy, and Graphic Arts IV,

G. B. Beretta, and R. Eschbach, Editors, Proc, of SPIE 3648, Bellingham, WA, 1999, pp. 218-225.

22. P. D. Burns and R. S. Berns, "Analysis of multispectral image capture", in IS&T/SID Fourth Color Imaging Conference: Color Science, Systems, and Applications, IS&T, Springfield, VA, 1996, pp. 19-22.

23. T. Jaaskelainen, J. Parkkinen and S. Toyooka, "Vector-subspace model for color representation", J. Opt. Soc. A, 7, 725-730, (1990).

24. L. T. Maloney, "Evaluation of linear models of surface spectral reflectance with small numbers of parameters", J. Opt. Soc. Am. A, 10, 1673-1683 (1986).

25. M. J. Vrhel, R. Gershon and L. S. Iwan, "Measurement and analysis of object reflectance spectra", Color Res. and Appl., 19, 4-9, (1994).

26. The New Munsell Student Color Set, Fairchild Publication, New York, 1994.

27. The collection at the National Gallery of Art, http://www.nga.gov./cgi-bin/pinfo?Object=106740+0+none

## Biography

Francisco H. Imai received his Ph.D. in imaging science from Chiba University, Japan in 1997. Since 1997 he has worked at Munsell Color Science Laboratory, Chester F. Carlson Center for Imaging Science, Rochester Institute of Technology where currently he is a senior color scientist. His research has been focused on multi-spectral color reproduction and spectral reconstruction. He was named as the recipient of the 1998 Itek Award for the best student paper in 1997 by IS&T. He is a member of the IS&T and the ISCC.